



The Society shall not be responsible for statements or opinions advanced in papers or in discussion at meetings of the Society or of its Divisions or Sections, or printed in its publications. Discussion is printed only if the paper is published in an ASME Journal. Released for general publication upon presentation. Full credit should be given to ASME, the Technical Division, and the author(s). Papers are available from ASME for nine months after the meeting.

Printed in USA.

Copyright © 1983 by ASME

AN INVESTIGATION OF THE ESTABLISHMENT OF A RECIRCULATION ZONE
BY SWIRLING FLOWS WITHIN A CONICAL DUCT

P. Rama Mohan
Lecturer in Mechanical Engineering
Regional Engineering College
Warangal 506 004 (A.P) India

C. M. Vara Prasad
Professor of Mechanical Engineering
Regional Engineering College
Warangal 506 004 (A.P) India

ABSTRACT

This paper reports an investigation carried out on the recirculation zones established in conical chambers with radial vane inlet swirlers. The boundaries of the recirculation zones established in various conical chambers of different cone angles are presented for different inlet swirl numbers and an optimum cone angle which gives a reasonably short length of the recirculation zone with maximum pressure recovery is suggested. The inlet swirl number is also optimized for a fairly high swirl strength within the recirculation zone and the inlet swirl number for which the recirculation completely disappears is also estimated. In addition to this, an equation is curve-fit to the experimental data which correlates the length of the recirculation zone for any given cone angle and inlet swirl number.

NOMENCLATURE

C	Magnitude of actual velocity of fluid
C_X	Component of velocity in the axial direction
C_r	Component of velocity in the radial direction
C_θ	Component of velocity in the tangential direction
C_{X0}	Axial velocity component at the axis, at the exit of the swirler
C_{XA}	Axial velocity component at the axis, at any axial station
C_r	Radial velocity at $r/R = 0.5$
C_θ	Tangential velocity component (or swirl velocity) at $r/R = 0.5$
D	Outside diameter of the swirler
r	Radial distance from the axis at any cross section
R	Radius of the chamber wall, at any cross section
S	Swirl number within the flow regime given by $(C_\theta/C_X) \times (r/R)$

Si Inlet swirl number given by $2/3$ of tangent of swirler vane angle
X Axial distance from the exit of the swirler
 X_Z Length of the recirculation zone
 α Cone angle of the conical chamber

1. INTRODUCTION

An important requirement of a gas turbine combustion chamber is to maintain a stable flame over a wide range of operating conditions. The most common technique adopted to achieve this goal is to establish a recirculation zone in the primary section of the combustion chamber by introducing the primary air through swirlers arranged at the inlet of the chamber. The pressure loss associated with the recirculating flow can be effectively recovered by providing a divergent shape for the combustion chamber.

It is experimentally established by Chigier et al. (1) that the axial length of the recirculation zone extends upto four orifice diameters of a swirl burner with a strong inlet swirl. Domkundwar (2) has experimentally investigated the effect of diffuser angle and equivalence ratio on stability characteristics, and based on the experimental data, he has proposed a model wherein the blow-off velocity is directly proportional to the equivalence ratio and tangent of the diffuser angle. Both Domkundwar (2) and Chigier et al. (1) employed the technique of axial and tangential air entry for the generation of recirculation zones and they reported relatively lower lengths of recirculation zone. In contrast to this, Beltagui et al. (3), while employing the technique of air entry through vane swirlers, has reported long lengths of recirculation zone of about seven swirler diameters with a 40° swirler. Hacker (4) used the mixing length theory of turbulence and developed a model for flames in swirling combustors. He concluded that the flame can be effectively

stabilized by controlling the swirl. Bafuwa et al.(5) have studied the effect of vane angle on the stability limits of a flame and reported that with an increase in vane angle, the blow-off velocity decreases. Pathi et al.(6) have investigated a recirculation zone established by vaned swirlers in a conical chamber of 43° cone angle. The length of recirculation zone as well as the negative swirl strength were found to increase with an increase in the swirler vane angle. However as this investigation was limited to a study on a single conical chamber it was found that there was a necessity to study the effects in more number of conical chambers with varying cone angles so that an optimum conical chamber matching an optimum inlet swirl number may be arrived at.

Hence a detailed analysis on five different conical chambers of varying cone angles is attempted in the present investigation employing radial vaned swirlers. An expression for the length of recirculation zone at any given cone angle and inlet swirl number is also developed based on the experimental data.

2. DESCRIPTION OF THE CONICAL COMBUSTOR

Fig.1 shows a dimensioned sketch of the conical test chamber assembled in the combustion chamber of a real gas turbine unit. The dimensions shown in the figure are for a typical test chamber of cone angle 33° fitted with a radial vaned swirler of hub and outer diameters equal to 8.2 and 25.4 mm. The conical shaped chamber covers the primary section and this is followed by a cylindrical shape of the chamber wherein the dilution and film-cooling air will be introduced.

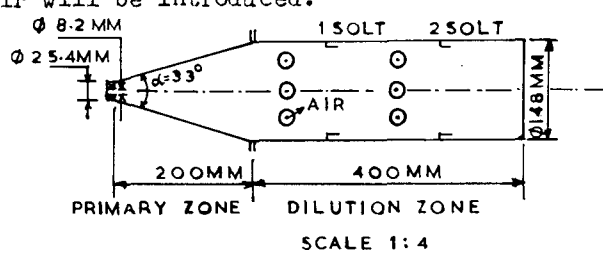


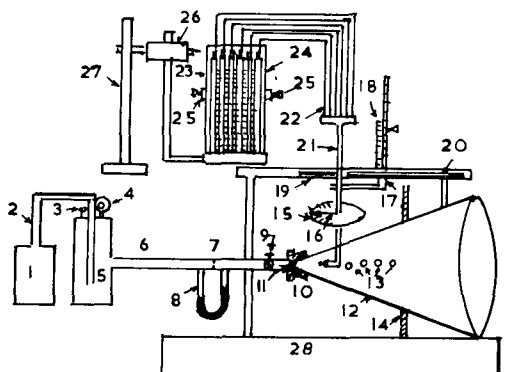
FIG.1 SKETCH OF THE CONICAL COMBUSTOR

3. EXPERIMENTAL SET-UP AND PROCEDURE

A schematic arrangement of the experimental set-up is shown in Fig.2.

The exhaust of a 4-cylinder Perkins diesel engine was used for the supply of necessary mass flows of gas through the conical chamber. Black smoke in the gas was eliminated by running the engine on no load and also by introducing a settling tank in the supply line. The gas temperature at inlet of the chamber was 50°C , and the flow velocity of gas was maintained in the range of 32.86 to 46.5 m/sec. The conical chamber was fitted with a radial vaned swirler at its inlet and the vane angle of different swirlers employed were in the range of 20° to 60° which correspond to inlet swirl number of 0.262 to 1.25. The swirler vane design was as per the recommendations of Mathur (7). A spherical pitot probe was first

calibrated by the usual procedure and was then used for the measurement of the three velocity components in the axial, radial and tangential directions at various points in the flow regime. The axial stations of the conical chamber at which the pitot probe was traversed were arranged at distances of 0.5, 1.0, 1.5, 2.0 and 3.0 times the swirler diameter from the inlet of the chamber. The end of recirculation zone, on the axis of the test chamber, was identified by traversing a tuft probe along the axis of the chamber and locating the point where the tuft indicated a change in the flow direction of the gas.



- 1. Engine
- 2. Exhaust pipe
- 3. Thermometer
- 4. Pressure gauge
- 5. Stabilizer tank
- 6. Supply pipe
- 7. Orifice
- 8. Manometer
- 9. Control valve
- 10. Flange
- 11. Swirler
- 12. Conical chamber
- 13. Axial stations
- 14. Side flanges
- 15. Protractor
- 16. Pointer
- 17. Mechanism for vertical traverse
- 18. Main and vernier scales
- 19. Mechanism for horizontal traverse
- 20. Slot
- 21. Probe
- 22. Probe connections
- 23. Multitube manometer
- 24. Frame
- 25. Manometer fixer
- 26. Tank
- 27. Stand
- 28. Table

FIG.2 SCHEMATIC OF THE EXPERIMENTAL SET-UP

4. DISCUSSION OF THE RESULTS

4.1 Distribution of the axial, radial and tangential velocity components

A typical inlet swirl number of 0.604, which is proved to be the optimum value by Pathi et al.(6), was selected for the presentation of data for discussion under this section.

Fig.3 presents the variation of non-dimensional axial velocity component with non-dimensional radial distance, at $X/D = 1.5$ and $S_i = 0.604$, and exhibits the nature of radial spread of the recirculation zone in the various conical chambers. The radial spread of the recirculation zone, with a negative axial velocity component, is increasing from 50% to 85% of the radial distance as the cone angle of the chamber increases from 23° to 63° . Better distribution of the zone in the radial direction, found in wider chamber, is due to a better opportunity for the fluid to diffuse in the radial direction.

Fig.4 presents the variation of non-dimensional radial velocity component with the non-dimensional radial distance, and shows that the flow is inward within the recirculation zone and it is outward outside the zone.

The variation of non-dimensional tangential velocity component with the non-dimensional radial distance is shown in Fig.5. The trend exhibited considerable oscillation from positive rotation to negative rotation. This trend is in agreement with the results presented by Chigier et al.(1) in swirling flows. Figs.6-8 present the variation of non-dimensional axial, radial and the tangential velocity components at different stations, along the axial distance of the conical chamber of 33° cone angle with an inlet swirl number of 0.604.

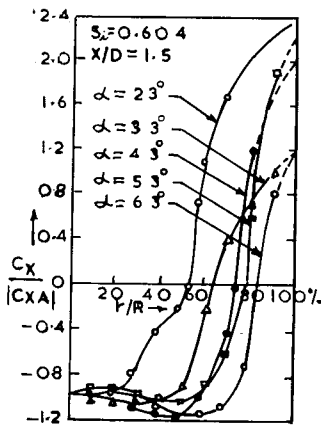


FIG.3 RADIAL PROFILES OF AXIAL VELOCITY

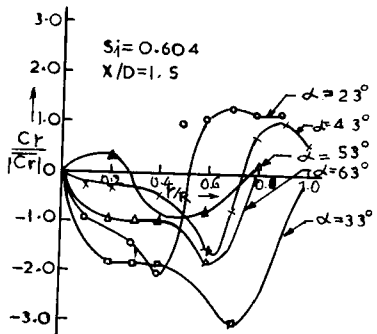


FIG.4 RADIAL PROFILES OF RADIAL VELOCITY

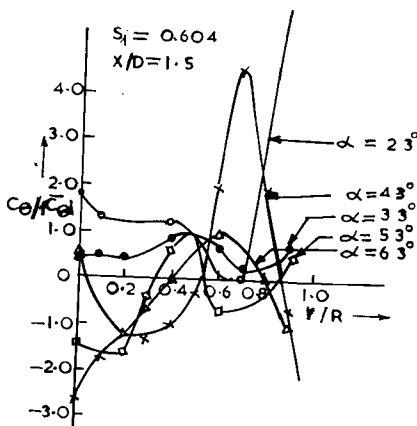


FIG.5 RADIAL PROFILES OF TANGENTIAL VELOCITY

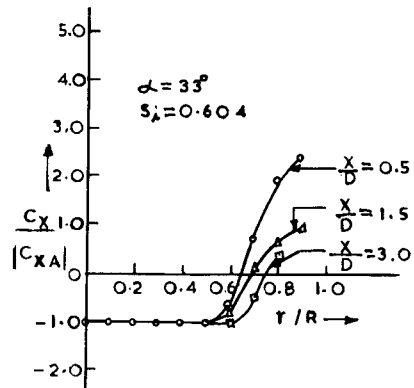


FIG.6 VARIATION OF AXIAL VELOCITY IN THE RADIAL DIRECTION FOR DIFFERENT AXIAL STATIONS

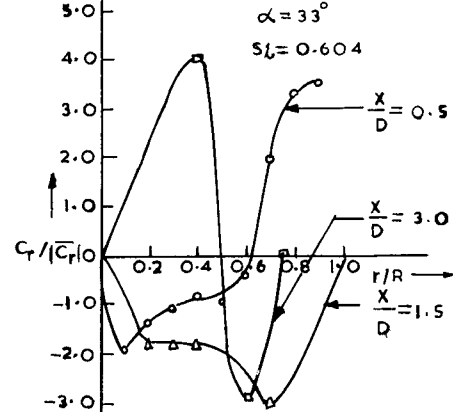


FIG.7 VARIATION OF RADIAL VELOCITY IN THE RADIAL DIRECTION FOR DIFFERENT AXIAL STATIONS

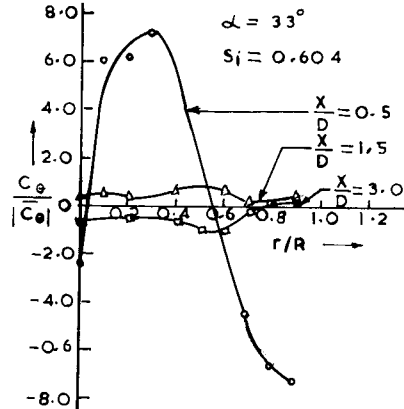
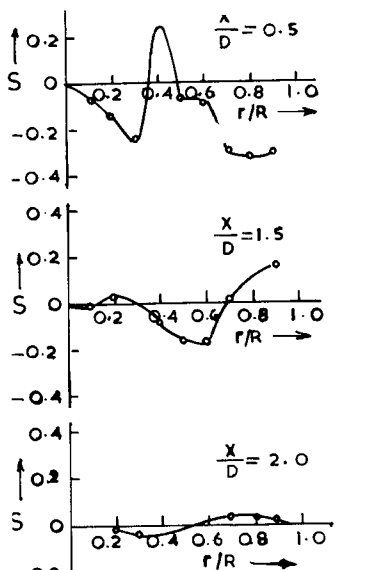


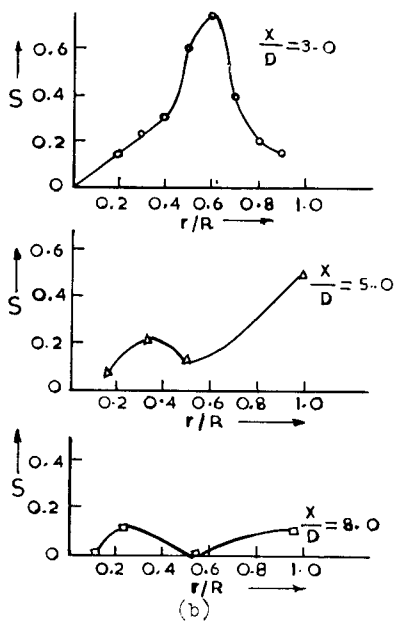
FIG.8 VARIATION OF TANGENTIAL VELOCITY IN THE RADIAL DIRECTION FOR DIFFERENT AXIAL STATIONS

4.2 Variation of swirl number

The variation of swirl number, S , given by $S = C_\theta/C_X (r/R)$, within the flow regime, is presented in Figs.9(a) and 9(b). The hub of the swirler blocks the entry of air at its centre. The axial momentum of air, just at the exit of the swirler, at its centre, is therefore zero. A low negative swirl is thus established at the axial station of $X/D = 0.5$, and at $X/D = 3.0$, the swirl is assuming a high positive value of 0.75 at $r/R = 0.6$. This swirl subsequently decays in the downstream direction and is almost zero at $X/D = 8.0$.



(a)



(b)

FIGS.9(a)&(b) SWIRL NUMBER VARIATION IN THE FLOW REGIME

Figs.10 and 11 are plotted with the idea of arriving at an optimum inlet swirl number which gives a reasonably high swirl strength at the axis of the chamber. Fig.10 presents the decay of swirl strength along the axis of the chamber for various inlet swirl numbers and Fig.11 shows the variation of swirl strength with the inlet swirl number for a typical axial station of $X/D = 1.5$. It can be seen from Fig.11 that the swirl strength increases at a fast rate of 1.0 unit per unit inlet swirl number, for S_i ranging from 0.262 to 0.6, while the rate of increase for higher inlet swirl numbers is of the order of 0.23 units. It is therefore concluded that an optimum value for the inlet swirl number which gives a reasonably high swirl strength is

around 0.6. This conclusion agrees with the results obtained by Pathi et al.(6) on a conical chamber and Ganeshan (8) on a can type chamber. Extrapolation of the curve of Fig.11 yields another important result that at an inlet swirl number of 0.2 the swirl strength is zero. This observation of the inlet swirl number at which the recirculation disappears is in agreement with that of Beltagui et al.(3).

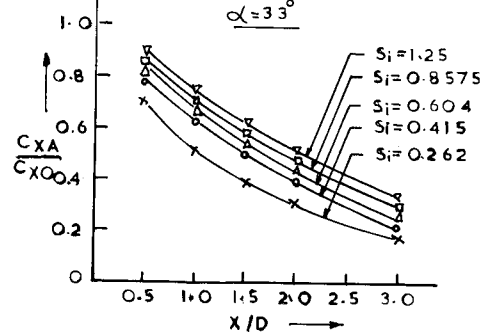


FIG.10 DECAY OF SWIRL STRENGTH ALONG THE AXIS FOR VARIOUS INLET SWIRL NUMBERS

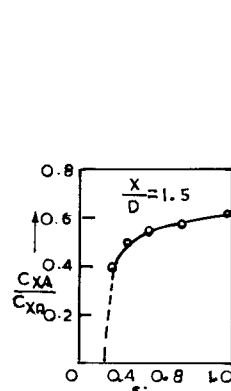


FIG.11 VARIATION OF SWIRL STRENGTH WITH INLET SWIRL NUMBER

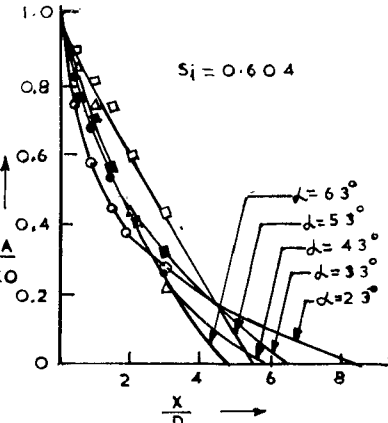


FIG.12 DECAY OF SWIRL STRENGTH ALONG THE AXIS FOR VARIOUS CONE ANGLES

4.3 Decay of the axial velocity component on the axis

Fig.12 is drawn to estimate the length of recirculation zone in a given conical chamber with a given inlet swirl number. The end of recirculation zone where the swirl strength becomes zero on the axis, is identified by means of tuft probe studies as explained in article 3. With the help of this data the curves of swirl strength have been extrapolated to meet the x-axis. Thus from this figure the lengths of recirculation zone have been determined for various cone angles.

4.4 Boundaries of the recirculation zone

The boundaries of recirculation zone in various conical chambers are presented in Fig.13. It can be clearly observed on the figure that for any given inlet swirl number, the length of recirculation zone decreases with an increase in the cone angle whereas the radial spread of the zone increases with an increase in the cone angle. There is a considerable reduction in the length of the zone for an increase in the cone angle from 23° to 33° .

whereas the reduction is marginal for a further increase right upto an angle of 63° . This fact is again evident from Fig.15 which is plotted to correlate the experimental results with analytical values. However, in a real gas turbine combustor, the coupling effect of dilution air which may entrain into the recirculation zone can bringin a reduction in the length of the recirculation zone. Moreover, under combusting conditions, the length of this zone is likely to get further reduced by about 50% as reported by Beltagui et al.(3) for a 30° -vaned swirler of annular type.

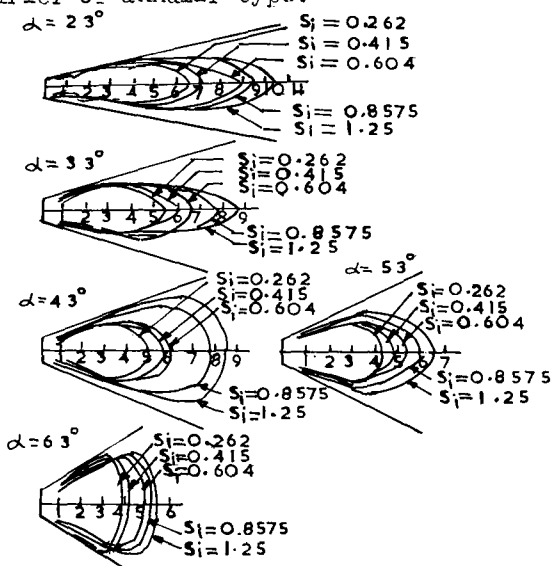


FIG.13 BOUNDARIES OF RECIRCULATION ZONE IN VARIOUS CONICAL CHAMBERS FOR DIFFERENT INLET SWIRL NUMBERS

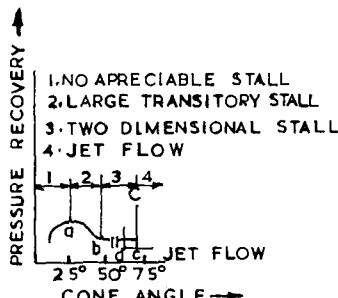


FIG.14 PRESSURE RECOVERY FOR VARIOUS CONE ANGLES

It can be observed from Fig.14 that for the swirl number of 0.604, the length of recirculation zone gets reduced by 33% when the cone angle is increased by 10° only (i.e., from 23° to 33°) whereas a further increase in the cone angle right upto 63° reduces the length by another 22% only. In addition, Heneau et al.(9) have established that for cone angles upto 30° , the pressure recovery will gradually increase and beyond 30° there is a reduction in the recovery factor. This fact is clearly exhibited in Fig.14. It can be therefore concluded that in view of a reasonably short length of the recirculation zone and a high pressure recovery, 30° is the optimum cone angle for the conical chamber.

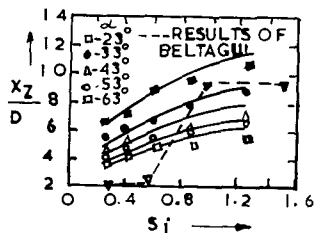


FIG.15 CORRELATION BETWEEN EXPERIMENTAL AND ANALYTICAL VALUES OF LENGTH OF RECIRCULATION ZONE

4.5 Comparison of data on length of recirculation zone with the work of other investigators

The variation of length of the recirculation zone with the inlet swirl number, as estimated by Beltagui et al.(3), is superimposed in Fig.15 for the sake of comparison with the results of the present work. The results of Beltagui et al. correspond to a cylindrical furnace employing hubless swirlers whereas those of the present investigation refer to annular type swirlers used in conical shaped chambers. Considering the can type chamber of Beltagui et al. as a chamber with cone angle of 180° , it can be seen from the figure, that at the optimum swirl number of 0.6, the results of Beltagui et al. exactly fit into the trend exhibited by the results of present investigation wherein the length of recirculation zone is gradually decreasing with an increase in the cone angle of the chamber. However for higher inlet swirl number, greater than 0.7, the correlation of can type chamber with conical chamber fails.

An error analysis of the entire experimental data is given in Appendix-1.

5. CURVEFIT OF THE EXPERIMENTAL DATA

The trend exhibited by plots of the swirl strength along the axis, for a given conical chamber, is found to fit into an equation of the form:

$$\left(\frac{X}{D} + a \right) \left(\frac{C_{XA}}{C_{X0}} + b \right) = \beta \quad (1)$$

where $\beta = a(1+b)$ and both 'a' and 'b' are functions of the inlet swirl number, S_i . The values of 'a', 'b' and ' β ' are evaluated by curve fitting and based on their variation with S_i , expressions have been developed (10) as functions of S_i for all these three quantities. Equation (1) therefore takes the form:

$$\frac{C_{XA}}{C_{X0}} = 1 + \frac{C_1 S_i (2 - S_i)^2}{X/D + C_2 S_i^{1.435} (2 - S_i)^{1.5}} - 1.725 S_i^{0.37} (2 - S_i)^{0.5} \quad (2)$$

wherein the values of C_1 and C_2 vary with the cone angle of the chamber as shown in Table-1.

Table - 1

Values of C_1 and C_2

(P.Rama Mohan et al.)

α	23°	33°	43°	53°	63°
C_1	12.90	10.23	8.36	7.728	6.42
C_2	7.49	5.93	4.85	4.480	3.72

The length of recirculation zone, non-dimensionalised as XZ/D , is now computed introducing the condition that $X/D = X_Z/D$ at $C_{XA}/C_{X0} = 0$.

Equation (2) therefore yields the following expression for X_Z/D :

$$\frac{X_Z}{D} = \frac{C_3 S_i^{1.485} (2 - S_i)^{1.5}}{1.725 S_i^{0.37} (2 - S_i)^{0.5} - 1} \quad (3)$$

with C_3 equal to 7.49, 5.93, 4.85, 4.48 and 3.72 as ' α ' goes from 23° - 63° . The curve of C_3 vs α is a rectangular hyperbola described by the equation:

$$C_3 = 50.2 (\alpha)^{-0.595}$$

and the most general expression for X_Z/D that follows from equation (3) is:

$$\frac{X_Z}{D} = \frac{50.2 S_i^{1.485} (2 - S_i)^{1.5} (\alpha)^{-0.595}}{1.725 S_i^{0.37} (2 - S_i)^{0.5} - 1} \quad (4)$$

A correlation between the experimental values and the predictions from equation (4) is presented in Fig.16 and a good agreement is observed between the two sets of values.

6. CONCLUSIONS

From the present investigation the following conclusions can be arrived at:

- (i) A conical chamber with an optimum cone angle of 33° gives a reasonably short length of the recirculation zone with an appreciable pressure recovery.
- (ii) A vaned swirler with an inlet swirl number of 0.6 produces a sufficiently high swirl strength.
- (iii) Equation (4) correlates the length of recirculation zone with sufficient amount of accuracy for the cone angles ranging from 23° to 63° and for the swirler vanes in the range of 20° to 60° .

REFERENCES

1. Chigier, R.A. et al., "Experimental Investigation of Swirling Vortex Motions in Jets", Trans. ASME, Ser. V, J. Appl. Mech., 34, p 443 (1967).
2. Domkundwar, J.M., "Effect of Diffuser on the Flame Stability in Swirling Jets", Proceedings of the 4th Biennial Seminar on Gas Turbines, Gas Turbine Research Establishment, Bangalore, p 507 (Nov.1979).
3. Beltagui, S.A. et al., "Aerodynamics of Vane Swirled Flames in Furnaces", J. Institute of Fuel, p 183 (Dec.1976).
4. Hacker, D.S., "A Simplified Mixing Length Model of Flame Stability in Swirling Combustors", AIAA Journal, p 65 (Jan.1974).
5. Bafuwa, C.C. and Maccallum, N.H.L., "Flame Stabilization in Swirling Jets", Combustion Institute of European Symposium, Sheffield, p 565 (1973).
6. Pathi, A.V.L. et al., "An Investigation on the Generation of Recirculation Zone by Combined Swirling Flows", Proceedings of the 4th National Conference on I.C. Engines and Combustion, p C2.29 (1977).
7. Mathur, M.L., "A New Design of Vanes for Swirl Generation", J. Instn. of Engineers (India), 55, pt ME2, p 93 (Nov.1974).
8. Ganesan, V., "Recirculation and Turbulent Studies in an Isothermal Model of a Gas Turbine Combustion Chamber", Ph.D. Thesis, Indian Institute of Technology, Madras (1974).
9. Henneau, L.R. et al., "Performance of Two-dimensional Diffusers", J. Basic Engineering, Ser. B, 89, 1, p 141 (March 1967).
10. Viswanatha Rao, A. et al., "Experimental Investigation on Swirl Generated Recirculation Zone in a Conical Combustion Chamber for Gas Turbine Application", Proceedings of the 4th Biennial Seminar on Gas Turbines, Gas Turbine Research Establishment, Bangalore, p 549 (Nov.1979).

APPENDIX-1
Error analysis of the experimental data
Fig.3

α	23°	33°	43°	53°	63°
Number of replications	9	10	9	10	10
Standard deviation	1.59	1.1	1.1	1.02	0.86

Fig.4

α	23°	33°	43°	53°	63°
Number of replications	9	5	9	4	5
Standard deviation	1.06	1.14	1.1	1.04	1.01

Fig.5

α	23°	33°	43°	53°	63°
Number of replications	4	7	8	7	7
Standard deviation	1.07	1.06	1.25	1.24	1.19

Fig.6

X/D	0.5	3.0
Number of replications	10	9
Standard deviation	1.20	1.17

Fig.7

X/D	0.5	3.0
Number of replications	10	5
Standard deviation	1.25	1.32

Fig.8

X/D	0.5	3.0
Number of replications	7	8
Standard deviation	1.78	1.73

Fig.9(a)

X/D	2.0	
Number of replications	5	
Standard deviation	1.69	

Fig.9(b)

X/D	5.0	8.0
Number of replications	4	4
Standard deviation	1.67	1.61

Fig.10

σ_i	1.25	0.8575	0.604	0.415	0.262
Number of replications	5	5	5	5	5
Standard deviation	0.216	0.205	0.204	0.204	0.208

Fig.12

α	23°	33°	43°	53°	63°
Number of replications	5	5	5	5	5
Standard deviation	0.202	0.197	0.196	0.198	0.201

The curves which are not covered above happen to be derived from the remaining figures.